Journal of
Nanoscience and Nanotechnology
Vol. 11, 8152–8157, 2011

TiO_2 Coating of High Surface Area Silica Gel by Chemical Vapor Deposition of $TiCl_4$ in a Fluidized-Bed Reactor

Wei Xia[1], Bastian Mei[1], Miguel D. Sánchez[1,2], Jennifer Strunk[1], and Martin Muhler[1,*]

[1] *Laboratory of Industrial Chemistry, Ruhr-University Bochum, 44780 Bochum, Germany*
[2] *Instituto de Física del Sur, Universidad Nacional del Sur-CONICET, 8000 Bahía Blanca, Argentina*

TiO_2 was deposited on high surface area porous silica gel (400 m^2g^{-1}) in a fluidized bed reactor. Chemical vapor deposition was employed for the coating under vacuum conditions with $TiCl_4$ as precursor. Nitrogen physisorption, X-ray diffraction, transmission electron microscopy, X-ray photoelectron spectroscopy and UV-vis spectroscopy were applied to characterize the obtained TiO_2–SiO_2 composites with different Ti loadings up to 5 wt%. Only a slight decrease in the specific surface area was detected at low Ti loadings. At a Ti loading of 2 wt%, TiO_2 was found to be highly dispersed on the SiO_2 surface likely in form of a thin film. At higher Ti loadings, two weak reflections corresponding to anatase TiO_2 were observed in the diffraction patterns indicating the presence of crystalline bulk TiO_2. High resolution XPS clearly distinguished two types of Ti species, i.e., Ti–O–Si at the interface and Ti–O–Ti in bulk TiO_2. The presence of polymeric TiO_x species at low Ti loadings was confirmed by a blue shift in the UV-vis spectra as compared to bulk TiO_2. All these results point to a strong interaction between the TiO_2 deposit and the porous SiO_2 substrate especially at low Ti loadings.

Keywords: TiO_2, Chemical Vapor Deposition, Fluidized-Bed Reactor, Strong Oxide–Oxide Interactions.

RESEARCH ARTICLE

1. INTRODUCTION

Silica gel is used as an acidic support for heterogeneous catalysts due to its favorable porosity and high stability. Under ambient conditions the surface of silica gel is saturated with hydroxyl groups, and its properties can be modified by doping with hetero-atoms such as Zr, Ti or Al. For example, Zr-containing mesoporous SiO_2 was found to be highly active in acid catalysis.[1] TiO_2–SiO_2 nanocomposites were used as support to obtain homogeneously distributed MoO_3 on the composite surface.[2] In the last decade, TiO_2 has attracted much attention in photocatalysis because of its high activity for water splitting under ultraviolet or visible light irradiation.[3] A large number of studies focused on the doping of TiO_2 to modify its band gap in order to modify its absorption properties, among which nitrogen doping is the most intensively investigated.[4,5] Recently, TiO_2–SiO_2 composites were used in photocatalysis and showed promising activities for methylene blue degradation.[6,7] The TiO_2–SiO_2 composite was also applied as support for Pt catalysts used in photocatalysis.[8]

The sol–gel method is the most commonly used method for the synthesis of TiO_2–SiO_2 hybrid nanocomposites.[9] Mesoporous TiO_2–SiO_2 aerogels with hierarchical pore structures were synthesized by the sol–gel method involving partial solvent evaporation and subsequent supercritical drying.[10] Chemical vapor deposition (CVD) in a fluidized-bed reactor is widely used for the coating of porous nanoparticles.[11,12] Fluidization can significantly enhance the homogeneity of the deposition by continuously mixing the support particles. Thin film coatings on porous substrates can be achieved by CVD without significant influence on the porosity of the substrate.[13] CVD was used for the deposition of TiO_2 on active carbon, silica gel and alumina substrate for photocatalytic applications.[14,15] Anatase TiO_2 were deposited on silica gel powders by plasma-enhanced CVD in a circulating fluidized-bed reactor, and the obtained nanocomposites were tested for photocatalytic degradation of methylene blue.[16]

Titanium compounds are typically air and water sensitive. Typical precursors for TiO_2 CVD include titanium nitrate $[Ti(NO_3)_4]$,[17] titanium isopropoxide $[Ti(OCH(CH_3)_2)_4]$,[18,19] titanium ethoxide

*Author to whom correspondence should be addressed.

1533-4880/2011/11/8152/006 doi:10.1166/jnn.2011.5107

$[Ti(OCH_2CH_3)_4]$,[20] and titanium tetrachloride $[Ti(Cl)_4]$.[21] Here, we report the coating of TiO_2 on high surface area porous silica gel in a fluidized-bed reactor. $TiCl_4$ was used as a carbon-free Ti precursor, and different loadings were achieved on silica.

2. EXPERIMENTAL DETAILS

Silica gel with an average pore size of 10 nm was obtained from Merck. Silica particles with the sieve fraction of 100–200 μm were used as substrate. Titanium tetrachloride (Fluka, >99.0%) was used as Ti precursor. For the fluidized-bed CVD a vertical quartz tube reactor and a glass evaporator installed in a drying oven were employed. The evaporation temperature was controlled by the oven, and a resistance heating wire was used for the heating of the fluidized-bed reactor. A vacuum pump was connected to the CVD system, and the pressure was adjusted in the range between 1 mbar and atmospheric pressure. The flow rate of all gases was controlled by mass flow controllers. Helium (purity 99.9999%) was used as carrier gas, and synthetic air (20.5% O_2 in N_2) was used as reaction gas.

In a typical experiment, 2 g of silica gel were loaded to the reactor (inner diameter 20 mm) resulting in a static bed height of about 11 mm. Before TiO_2 deposition, the silica gel as well as the CVD system was dried under helium flow (100 sccm) by keeping the oven temperature at 110 °C and the reactor temperature at 200 °C (through additional heating wire) for 60 min. After drying, the silica substrate was heated to 400 °C at 10 K/min, and the oven was turned off for cooling. Helium (100 sccm) as carrier gas was then passed through the evaporator and synthetic air (100 sccm) was passed through the reactor. Subsequently, a pre-determined amount of $TiCl_4$ precursor was injected into the evaporator using an autoclavable pipette. After purging the evaporator by flowing helium (100 sccm) for about 5 min to remove air, the oven was heated to 75 °C for the evaporation of $TiCl_4$. Simultaneously, the system pressure was slowly lowered to 400 mbar. The silica particles were in the fluidized state under these conditions. The evaporation took no more than 30 min depending on the amount of the $TiCl_4$ precursor. Subsequently, the pressure was released and the sample was calcined in fixed-bed under flowing air (100 sccm) at 400 °C for 120 min.

Elemental analysis was performed using a Pye Unicam 7000 ICP-OES spectrometer. X-ray diffraction (XRD) was carried out with a Philips X-Pert MPD system with CuKα radiation. X-ray photoelectron spectroscopy (XPS) measurements were carried out in an ultra-high vacuum set-up equipped with a Scienta Gammadata SES2002 analyser. The base pressure in the measurement chamber was 5×10^{-10} mbar. Monochromatic AlKα (1486.6 eV) was used as incident radiation and a pass energy of 200 eV was applied for region measurements. Charging effects were compensated by a flood gun. Since Si and O are the dominating elements on the surface, the spectra were calibrated using Si 2p peaks by setting the main peak at 103.6 eV corresponding to Si in SiO_2. For comparison all the spectra were normalized by the intensity of corresponding Si 2p peak. The BET surface areas were determined by nitrogen adsorption at 77 K. The samples were out-gassed at 300 °C, until the pressure was lower than 500 Pa. The apparent surface density of Ti, expressed in Ti atoms per nm^2, was then calculated from the Ti loading and the BET surface area. Transmission electron microscopy was carried out with a Philips CM 200 FEG system. UV-vis spectra were recorded in the diffuse reflectance mode in a Perkin Elmer Lambda 650 UV-Vis spectrometer equipped with a Praying-Mantis mirror construction. The obtained spectra were converted by the Kubelka-Munk function $F(R)$ into absorption spectra using $BaSO_4$ as white standard.

3. RESULTS AND DISCUSSION

$TiCl_4$ is a strong Lewis acid easily hydrolyzing upon contact with air or moisture to release HCl, which immediately absorbs water to form droplets of hydrochloric acid. However, a fast transfer using an autoclavable pipette allowed us to load the $TiCl_4$ precursor to the saturator without significant material loss. The silica gel used as substrate is classified as a Geldart type B powder and can be easily fluidized.[22] The fluidization of silica particles was achieved by adjusting the flow rate of the feed gas at appropriate temperatures and pressures.

Different amount of precursors were applied corresponding to desired Ti loadings in the range from 2 to 10 wt%. Elemental analysis shows that the Ti yield is relatively high at loadings lower than 6 wt% (Table I). However, at higher loadings of 8 wt% and 10 wt% based on the amount of Ti precursor, the actually achieved Ti loading was found to be about 5 wt%, and it was not possible to reach even higher Ti loadings. The apparent surface density of Ti (atoms per nm^2) was derived from the Ti loading and the corresponding BET surface area (Table I). The obtained apparent loadings of around 1.5 Ti/nm^2 are still lower than the monolayer capacity of 4 Ti/nm^2 reported

Table I. Elemental analysis and nitrogen physisorption results of TiO_2–SiO_2 composite samples synthesized by CVD. The substrate SiO_2 was included for comparison. The apparent surface density of Ti was calculated from the Ti loading and the BET surface area.

Sample	Desired loading (Ti wt%)	Real loading (Ti wt%)	Apparent surface density of Ti (atoms nm^{-2})	BET (m^2 g^{-1})	Pore volume (cm^3 g^{-1})
SiO_2	0	0	0	400.5	0.781
TiSi-2	2	1.93	0.61	396.6	0.756
TiSi-4	4	4.17	1.31	382.6	0.699
TiSi-6	6	4.98	1.56	364.2	0.682

by Wong and coworkers.[25] However, in a study of titania grafted onto MCM-48, it was found that the maximum of Ti that can be bound to the silica surface in one step did not exceed 1 Ti/nm^2 possibly due to a lack of anchoring sites for the precursor.[26] It is known that hydroxyl groups on the silica surface are the anchoring sites for foreign species.[23] Hence, the upper limit of Ti loading in the one-step synthesis is assumed to be related to the amount of active sites on the silica surface. A detailed study is under way to determine the exact amount of hydroxyl groups, which will be correlated to the amount of deposited TiO_2 to verify the upper limits. The specific surface area of the silica substrate was determined to be 400.5 m^2g^{-1}. The deposition of TiO_2 did not cause a significant decrease in the surface area especially at low Ti loadings, as can be seen from Table I. The nitrogen physisorption investigations did not show significant decreases of the pore volume especially at low Ti loadings, which indicates that the pores of the silica particles were mostly not blocked by the TiO_2 deposits.

The XRD patterns of the TiO_2–SiO_2 samples are shown in Figure 1. The silica substrate shows a background with broad contributions at lower diffraction angles. With 2 wt% TiO_2 the diffraction pattern differs hardly from the silica substrate indicating the absence of crystalline TiO_2. Two weak reflections at around $2\theta = 25.5°$ and $2\theta = 48.2°$ appeared in samples with higher Ti loadings (sample TiSi-4 and TiSi-6). The two peaks are characteristic for anatase TiO_2 indicating the presence of bulk TiO_2. The crystallites are obviously rather small, because the reflections are very weak.

To determine the morphology and structure of the TiO_2–SiO_2 deposits, the samples were investigated by TEM. All the samples show very similar features (Fig. 2), and clear differences between the composites and the silica substrate were not observed. Even at a high Ti loading of 4.98 wt%, the sample TiSi-6 looks rather homogeneous and a clear phase contrast was not observed. Hence,

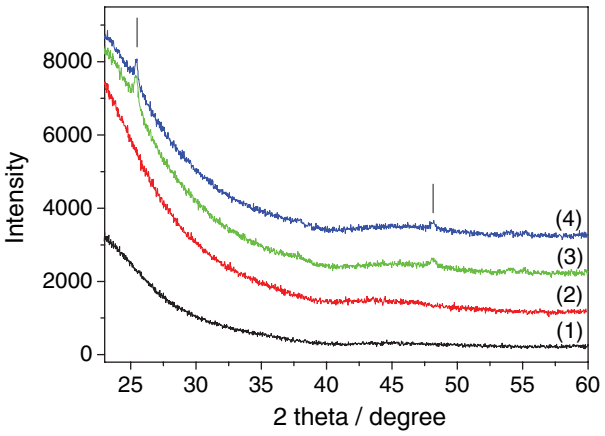

Fig. 1. XRD patterns of the silica substrate and TiO_2–SiO_2 composites with different Ti loadings. (1) SiO_2; (2) TiSi-2; (3) TiSi-4; (4) TiSi-6.

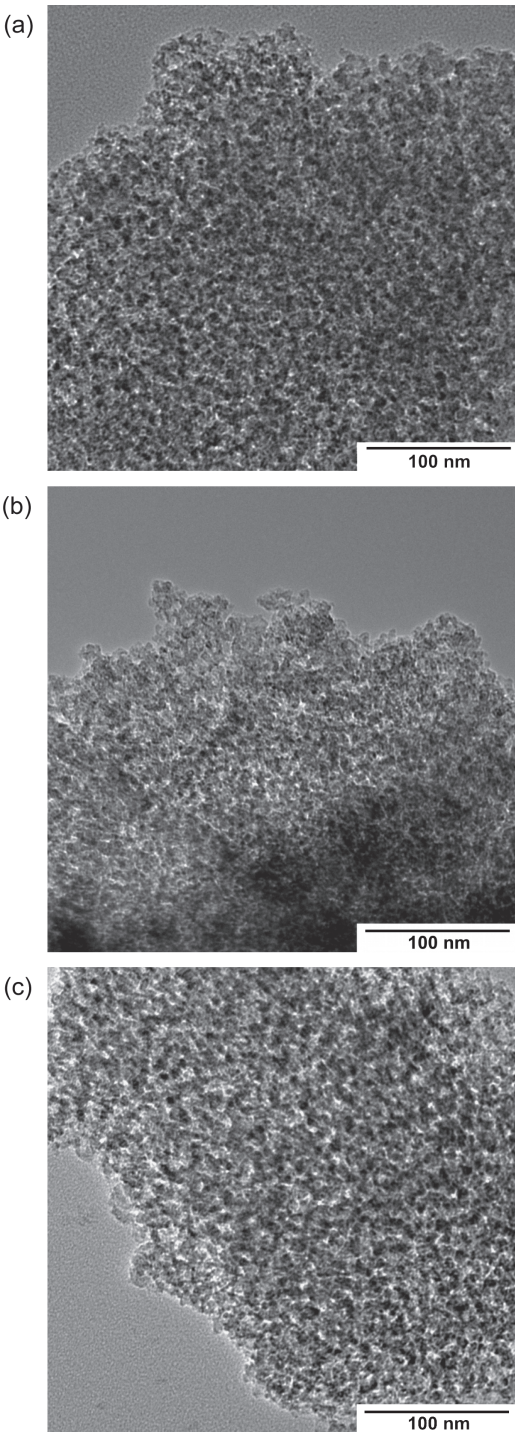

Fig. 2. TEM images of TiO_2–SiO_2 composite. (a) TiSi-2; (b) TiSi-4; (c) TiSi-6.

the formation of large TiO_2 particles or agglomerates is not likely, which is in agreement with the XRD results. However, the presence of small nanoparticles cannot be excluded by the TEM results.

X-ray photoelectron spectroscopy was applied to characterize the TiO_2–SiO_2 composites. Since Si and O are the dominating elements on the surface, the spectra were

calibrated using the Si 2p peaks by setting the main peak at 103.6 eV corresponding to Si in SiO_2. For comparison, all the spectra were normalized by the intensity of the corresponding Si 2p peak. The Si 2p spectra are typical for Si in SiO_2 (Fig. 3(a)). With increasing Ti loading, the Si 2p spectra did not show obvious change in symmetry. As expected, the main peaks of the O 1s spectra of all the four samples appear at the same position after calibration

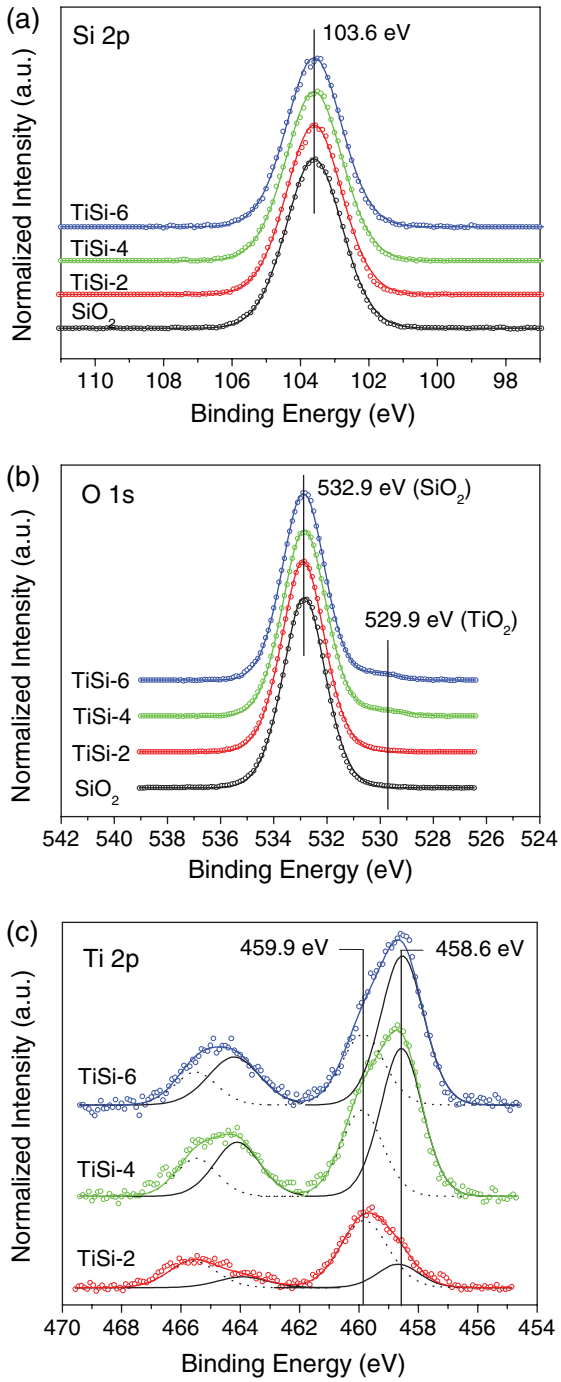

Fig. 3. XP spectra of the SiO_2 substrate and the TiO_2–SiO_2 composites with different Ti loadings. (a) Si 2p; (b) O 1s; (c) Ti 2p.

with Si 2p (Fig. 3(b)). The main peak at 532.9 eV can be assigned to oxygen in SiO_2, which is the dominating oxygen species on the surface of the composites. With increasing Ti loading, a weak peak appears at the lower binding energy side of the main O 1s peak. The weak contribution at 529.9 eV originates from oxygen in TiO_2. Different from the Si 2p and O 1s peaks, both the Ti $2p_{3/2}$ and $2p_{1/2}$ peaks show clear shifts to lower binding energies with increasing Ti loadings (Fig. 3(c)). Fitting of the Ti $2p_{3/2}$ peak resolved two contributions at 459.9 eV and 458.6 eV. A low binding energy shoulder at around 457 eV is often observed in doped TiO_2 samples, which can be assigned to Ti(III) species.[24] Obviously, this is not the case in the composite samples. The peak at 458.6 eV corresponds to Ti(IV) in bulk TiO_2 and the higher binding energy peak at 459.9 eV can be assigned to Ti–O–Si species. The shift of the peak to higher binding energy points to a strong interaction between the TiO_2 coating and the SiO_2 substrate. At lower TiO_2 loadings (e.g., sample TiSi-2 in Fig. 3(c)), Ti–O–Si species dominate the composite interface corresponding to a significantly higher contribution at 459.9 eV than at 458.6 eV (bulk TiO_2). With increasing Ti loading, the high binding energy peak remains roughly unchanged, whereas the peak at lower binding energy increased considerably. Obviously, the amount of bulk TiO_2 increases with increasing Ti loadings in agreement with the XRD results.

The surface compositions are derived from these XPS results and summarized in Table II. As expected, Si and O are the dominating species in the composites. Both the Si and O concentrations decrease slightly with increasing Ti loadings. The Ti surface atomic concentration of sample TiSi-2 was determined to be 0.5%, which increased to 1.2% for sample TiSi-4 and TiSi-6. A comparison of the XPS surface atomic concentration and the weight loading of Ti is shown in Figure 4. It can be seen that the surface Ti atomic concentration and the Ti weight loading are linearly correlated (Fig. 4). A slightly deviation can be observed for the high loading sample TiSi-6. The linear dependence indicates that the TiO_2 species are highly dispersed on the SiO_2 surface especially at low Ti loadings.

The optical absorption properties of the composites were studied by UV-vis spectroscopy (Fig. 5). UV-vis spectroscopy has been applied to characterize the degree of surface coverage of TiO_2 on SiO_2.[25] As compared to bulk

Table II. Surface compositions of the TiO_2–SiO_2composite samples with different Ti loadings derived from XPS.

	Atomic concentration (%)			
Sample	Si	O	Ti	Ti to Si ratio
SiO_2	28.6	71.4	–	–
TiSi-2	28.0	71.5	0.5	0.019
TiSi-4	27.9	70.9	1.2	0.043
TiSi-6	27.9	70.9	1.2	0.043

RESEARCH ARTICLE

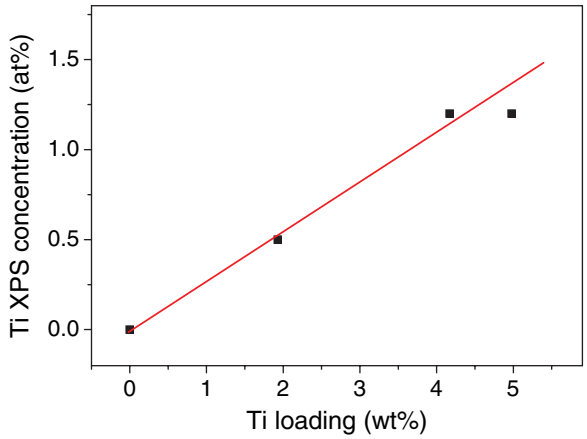

Fig. 4. XPS surface atomic concentration of Ti as a function of the Ti weight loading derived from elemental analysis. A linear fitting was applied to the data.

TiO_2, isolated TiO_2 species at extremely low Ti coverage showed significantly different absorption behaviour leading to UV-vis edge energies as high as 4.3 eV.[26] Edge energies around 3.4 eV can be assigned to polymeric TiO_x chains.[25] As can be seen from Figure 5, the absorption spectra of the TiO_2–SiO_2 samples show small but clear shifts. With increasing Ti loading, the spectra shifted to higher wavelength. The calculated edge energies of the three samples are 3.35 eV, 3.22 eV, and 3.19 eV for TiSi-2, TiSi-4, and TiSi-6, respectively. The higher edge energy of 3.35 eV of sample TiSi-2 may be assigned to polymeric TiO_x chains. The edge energies of TiSi-4 and TiSi-6 fit well to bulk anatase TiO_2, which has an edge energy of 3.2 eV.[26] The presence of polymeric TiO_x observed in sample TiSi-2 indicates a strong interaction between the deposited species and the substrate due to the presence of Ti–O–Si bonds, which can be clearly distinguished from Ti–O–Ti in bulk TiO_2 (sample TiSi-4 and TiSi-6). Hence, the UV-vis results further confirmed a strong interaction between TiO_2 and SiO_2 especially at low Ti loadings.

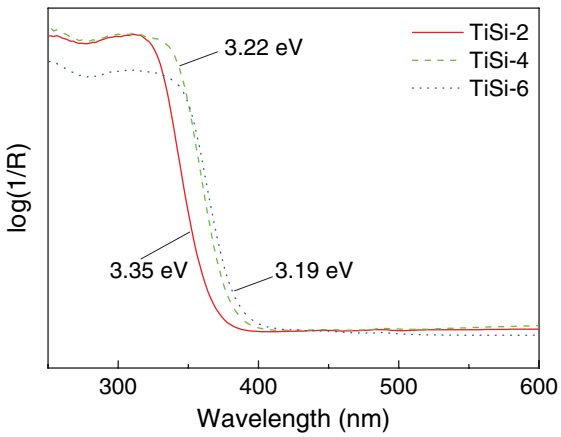

Fig. 5. UV-vis spectra of TiO_2–SiO_2 composites with different Ti loadings. The calculated edge energies are given for quantitative comparison.

4. CONCLUSIONS

TiO_2 was deposited on high surface area porous silica gel by CVD in a fluidized bed reactor using $TiCl_4$ as precursor. The obtained composite samples were characterized by nitrogen physisorption, TEM, XRD, high resolution XPS, and UV-vis. It was found that TiO_2 was highly dispersed on SiO_2 surface likely in form of thin films at low Ti loadings. Bulk TiO_2 was detected at Ti loadings exceeding 4 wt%. Two different Ti species were clearly distinguished by XPS and UV-vis spectroscopy, i.e., Ti–O–Si at the interface and Ti–O–Ti in the bulk of TiO_2. All these results point to a strong interaction between the TiO_2 deposit and the porous SiO_2 substrate especially at low Ti loadings.

Acknowledgments: This work was supported by the German Research Foundation (Deutsche Forschungsgemeinschaft) under project MU 1327/5-1.

References and Notes

1. A. O. Bianchi, M. Campanati, P. Maireles-Torres, E. Rodriguez Castellon, A. Jimenéz López, and A. Vaccari, *Appl. Catal. A* 220, 105 (**2001**).
2. B. M. Reddy, B. Chowdhury, and P. G. Smirniotis, *Appl. Catal. A* 211, 19 (**2001**).
3. M. K. Nowotny, L. R. Sheppard, T. Bak, and J. Nowotny, *J. Phys. Chem. C* 112, 5275 (**2008**).
4. H. Irie, Y. Watanabe, and K. Hashimoto, *J. Phys. Chem. B* 107, 5483 (**2003**).
5. M. Mrowetz, W. Balcerski, A. J. Colussi, and M. R. Hoffmann, *J. Phys. Chem. B* 108, 17269 (**2004**).
6. L. Luo, A. T. Cooper, and M. Fan, *J. Hazardous Mater.* 161, 175 (**2009**).
7. M. Zhang, L. Shi, S. Yuan, Y. Zhao, and J. Fang, *J. Colloid Interface Sci.* 330, 113 (**2009**).
8. X. Zhang, H. Yang, F. Zhang, and K.-Y. Chan, *Mater. Lett.* 61, 2231 (**2007**).
9. T. Ohno, S. Tagawa, H. Itoh, H. Suzuki, and T. Matsuda, *Mater. Chem. Phys.* 113, 119 (**2009**).
10. N. Yao, S. Cao, and K. L. Yeung, *Microporous Mesoporous Mater.* 117, 570 (**2009**).
11. C. Vahlas, B. Caussat, P. Serp, and G. N. Angelopoulos, *Mater. Sci. Eng. R-Rep.* 53, 1 (**2006**).
12. X. Mu, U. Bartmann, M. Guraya, G. W. Busser, U. Weckenmann, R. Fischer, and M. Muhler, *Appl. Catal. A* 248, 85 (**2003**).
13. W. Xia, Y. Wang, V. Hagen, A. Heel, G. Kasper, U. Patil, A. Devi, and M. Muhler, *Chem. Vap. Deposition* 13, 37 (**2007**).
14. G. L. Puma, A. Bono, D. Krishnaiah, and J. G. Collin, *J. Hazardous Mater.* 157, 209 (**2008**).
15. Z. Ding, X. J. Hu, P. L. Yue, G. Q. Lu, and P. F. Greenfield, *Catal. Today* 68, 173 (**2001**).
16. G. H. Kim, S. D. Kim, and S. H. Park, *Chem. Eng. Process.* 48, 1135 (**2009**).
17. C. J. Taylor, D. C. Gilmer, D. G. Colombo, G. D. Wilk, S. A. Campbell, J. Roberts, and W. L. Gladfelter, *J. Am. Chem. Soc.* 121, 5220 (**1999**).
18. G. A. Battiston, R. Gerbasi, A. Gregori, M. Porchia, S. Cattarin, and G. A. Rizzi, *Thin Solid Films* 371, 126 (**2000**).
19. S. Seifried, M. Winterer, and H. Hahn, *Chem. Vap. Deposition* 6, 239 (**2000**).

RESEARCH ARTICLE

20. A. Rahtu, K. Kukli, and M. Ritala, *Chem. Mater.* 13, 817 **(2001)**.
21. V. Gunko, V. Bogatyrev, V. V. Turov, R. Leboda, J. Skubiszewska-Zieba, L. V. Petrus, G. R. Yurchenko, O. I. Oranska, and V. A. Pokrovsky, *Powder Technol.* 164, 153 **(2006)**.
22. O. Molerus, *Powder Technol.* 33, 81 **(1982)**.
23. A. O. Bouh, G. L. Rice, and S. L. Scott, *J. Am. Chem. Soc.* 121, 7201 **(1999)**.
24. D. Morris, Y. Dou, J. Rebane, C. E. J. Mitchell, R. G. Egdell, D. S. L. Law, A. Vittadini, and M. Casarin, *Phys. Rev. B* 61, 13445 **(2000)**.
25. E. I. Ross-Medgaarden, I. E. Wachs, W. V. Knowles, A. Burrows, C. J. Kiely, and M. S. Wong, *J. Am. Chem. Soc.* 131, 680 **(2008)**.
26. J. Strunk, W. C. Vining, and A. T. Bell, *J. Phys. Chem. C* 114, 16937 **(2010)**.

Received: 9 May 2011. Accepted: 15 June 2011.